BIOCHEMISTRY

Proximity biotinylation identifies a set of conformation-specific interactions between Merlin and cell junction proteins

Robert F. Hennigan[1]*, Jonathan S. Fletcher[1], Steven Guard[2], Nancy Ratner[1]

Neurofibromatosis type 2 is an inherited, neoplastic disease associated with schwannomas, meningiomas, and ependymomas and that is caused by inactivation of the tumor suppressor gene *NF2*. The *NF2* gene product, Merlin, has no intrinsic catalytic activity; its tumor suppressor function is mediated through the proteins with which it interacts. We used proximity biotinylation followed by mass spectrometry and direct binding assays to identify proteins that associated with wild-type and various mutant forms of Merlin in immortalized Schwann cells. We defined a set of 52 proteins in close proximity to wild-type Merlin. Most of the Merlin-proximal proteins were components of cell junctional signaling complexes, suggesting that additional potential interaction partners may exist in adherens junctions, tight junctions, and focal adhesions. With mutant forms of Merlin that cannot bind to phosphatidylinositol 4,5-bisphosphate (PIP_2) or that constitutively adopt a closed conformation, we confirmed a critical role for PIP_2 binding in Merlin function and identified a large cohort of proteins that specifically interacted with Merlin in the closed conformation. Among these proteins, we identified a previously unreported Merlin-binding protein, apoptosis-stimulated p53 protein 2 (ASPP2, also called Tp53bp2), that bound to closed-conformation Merlin predominately through the FERM domain. Our results demonstrate that Merlin is a component of cell junctional mechanosensing complexes and defines a specific set of proteins through which it acts.

INTRODUCTION

Neurofibromatosis type 2 (NF2) is an inherited neoplastic disease characterized by slow-growing tumors, schwannomas, meningiomas, and ependymomas that are refractory to conventional chemotherapy (*1*–*3*). The tumor suppressor gene mutated in this disorder, *NF2*, is also inactivated in spontaneously arising schwannomas and malignant mesothelioma (*4*). Targeted deletion of *Nf2* in mouse Schwann cells leads to tumor formation (*5*, *6*). *Nf2*-null cells have a subtle phenotype in vitro, characterized by high cell density and impaired contact inhibition of growth (*7*).

The *NF2* gene encodes Merlin, a 70-kDa member of the ezrin-radixin-moesin (ERM) branch of the band 4.1 superfamily (*8*). ERM proteins have a conserved domain structure consisting of an N-terminal FERM (4.1, ERM) domain, a central α-helical region, and a C-terminal domain (CTD) (*9*). Like that of other ERM proteins, the central α-helical domain of Merlin folds over itself to form an antiparallel coiled coil that juxtaposes the CTD against the FERM domain (*10*). This orientation stabilizes the CTD in position to engage in low-affinity interactions with the FERM domain (*11*), thereby controlling access to binding sites. Shifts in orientation of the CTD relative to the FERM domain yield "open" conformations in which the FERM domain is accessible and "closed" conformations in which the FERM domain is inaccessible (*12*–*14*).

In myelinating Schwann cells, Merlin is localized to Schmidt-Lantermann incisures and paranodes, which are specialized regions containing junctional structures analogous to epithelial adherens and tight junctions (*15*, *16*). In cultured cells, Merlin localizes predominately to the inner face of the plasma membrane (*15*, *17*). A portion of Merlin associates with lipid rafts, cholesterol- and glycosphingolipid-rich membrane domains that have high concentrations of signaling molecules (*18*). Lipid raft association is mediated by binding to phosphatidylinositol 4,5-bisphosphate (PIP_2) and is necessary for Merlin-mediated growth suppression in vitro (*14*, *19*). Most of the literature shows that Merlin tumor suppressor functions are performed at the cytosolic face of the plasma membrane (*20*–*25*).

Merlin-deficient cells show activation of oncogenic signaling pathways including Rac, Src, β-catenin, and Ras (*26*–*31*), and some publications suggest that Merlin promotes contact inhibition by reducing the cell surface availability of growth factor receptors such as ErbB2, E-cadherin, and the epidermal growth factor receptor (*20*, *32*). Merlin has been implicated in intracellular vesicular trafficking, including growth factor endocytosis and exocytosis (*21*, *22*, *33*–*36*). Merlin binds to the tight junction protein Angiomotin, and this interaction inhibits Rac1 activity (*37*). Merlin is also detected in the nucleus (*38*, *39*), where it is reported to mediate contact inhibition and suppress tumorigenesis by inhibiting the E3 ubiquitin ligase $CRL4^{DCAF1}$ (*40*, *41*). Merlin is an activator of the Hippo pathway, a growth inhibitory kinase cascade that phosphorylates the growth-promoting transcription factor YAP1, thereby targeting it for degradation (*42*–*46*). The literature regarding Merlin function is complex and often contradictory, leading to poor understanding of the molecular mechanisms by which Merlin acts as a tumor suppressor.

Because Merlin has no known catalytic activity, its function is defined by the proteins with which it interacts. More than 30 interacting proteins have been described for Merlin (*47*), using either conventional pull-down assays or two-hybrid systems. Although many of these proteins have roles in oncogenic signal transduction, there is no consensus about which interactions are critical for tumor suppression. To better understand Merlin function, we conducted a census of Merlin interactions in Schwann cells using proximity biotinylation, a global proteomic analytic tool that identifies proteins that interact with, or are in close proximity to, Merlin. We defined

[1]Division of Experimental Hematology and Cancer Biology, Cincinnati Children's Hospital, Cincinnati, OH 45229, USA. [2]Department of Molecular, Cellular & Developmental Biology, University of Colorado Boulder, Boulder, CO 80309, USA.
*Corresponding author. Email: robert.hennigan@cchmc.org

a set of 52 Merlin-associated proteins, including known Merlin-binding proteins such as Angiomotin and Erbin. Using mutant Merlin proteins, we identified cohorts of Merlin-proximal proteins that depend on Merlin binding to PIP_2, interact with the Merlin CTD, or are specific for the closed conformation of Merlin. Most of the Merlin-proximal proteins function at the interface between the actin cytoskeleton and cell junctions, particularly in tight and adherens junctions, consistent with a critical role for Merlin in mechanosensory signal transduction pathways in peripheral nerve Schwann cells (*16*, *48*–*50*).

RESULTS

Proximity biotinylation and mass spectrometry identify Merlin-associated proteins

We performed proximity biotinylation by fusing Merlin to a mutant form of the *Escherichia coli* biotin ligase, $BirA^{R118G}$. This mutant has a substitution in the catalytic core that allows the active intermediate, biotin-5′–adenosine monophosphate to diffuse away, thereby biotinylating proteins in close proximity to the Merlin-BirA fusion (*51*). We generated stable populations of immortalized murine *Nf2*$^{-/-}$ Schwann cells (*5*) expressing Merlin fused to $BirA^{R118G}$ at its C terminus (Merlin-$BirA^{R118G}$) under the control of a doxycycline (Dox)–inducible promoter (fig. S1, A to F). To control for positional effects, we also generated a cell line expressing $BirA^{R118G}$ fused to the N terminus of Merlin ($BirA^{R118G}$-Merlin; Fig. 1A). To investigate potential changes in Merlin's interactome when bound to PIP_2, we fused $BirA^{R118G}$ to the C terminus of Merlin-6N (Merlin-6N–$BirA^{R118G}$; Fig. 1A), a mutant that does not bind phosphoinositides, localize to membrane lipid rafts, or inhibit cell growth (*19*). Because Merlin function is thought to be regulated by conformational changes that allow the CTD to control access to binding sites in the FERM domain, we constructed a deletion mutant containing only the FERM and helix domains and missing the CTD, Merlin-FH–$BirA^{R118G}$, which is expected to identify proteins that bind to the open, FERM-accessible conformation or require the CTD for interaction (Fig. 1A). We also constructed a cell line expressing Merlin-AR–$BirA^{R118G}$ (Fig. 1A), containing two point mutations in the CTD, A585W and R588K, that stabilize the interaction of the CTD with the FERM domain, thus mimicking a closed, FERM-inaccessible conformation (*52*). As a negative control, we used a cell line expressing $BirA^{R118G}$ fused to an unrelated protein, A-fos ($BirA^{R118G}$–A-fos). A-fos was used because it is present in cells in similar amounts as Merlin, has both cytoplasmic and nuclear localization, and binds tightly to Jun, thus providing an internal control for proximal biotinylation.

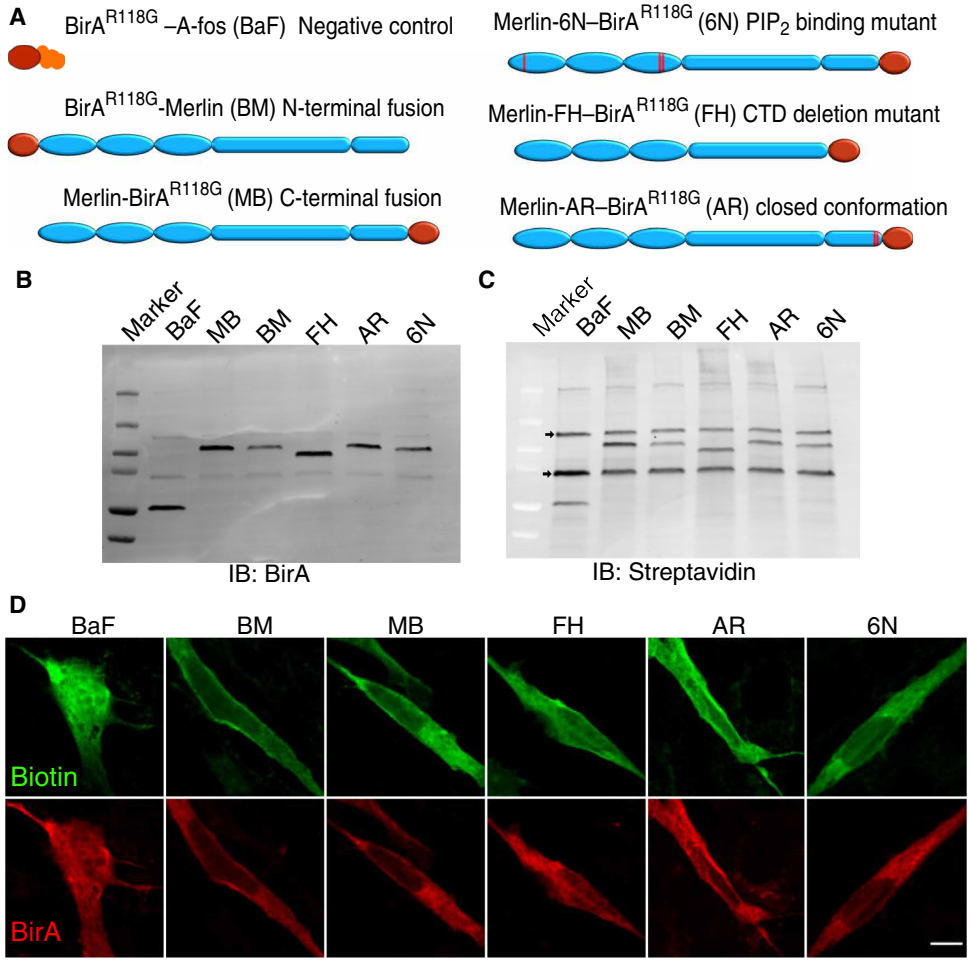

Fig. 1. Proximity biotinylation constructs. (**A**) A schematic diagram depicting the six $BirA^{R118G}$ fusion constructs expressed from Dox-inducible plasmids in immortalized *NF2*$^{-/-}$ mouse Schwann cells. Constructs include a negative control ($BirA^{R118G}$–A-fos), two wild-type Merlin constructs with BirA fused to either the N or C terminus ($BirA^{R118G}$-Merlin and Merlin-$BirA^{R118G}$), a PIP_2 binding–deficient mutant (Merlin-6N–$BirA^{R118G}$), a C-terminal deletion mutant intended to mimic the open, FERM-accessible conformation (Merlin-FH–$BirA^{R118G}$), and a mutant intended to mimic a closed, FERM-inaccessible conformation (Merlin-AR–$BirA^{R118G}$). (**B** and **C**) Immunoblotting (IB) of cell lysates from Dox-induced cells, probed with antibodies directed against BirA (B) or with streptavidin (C) to visualize biotinylated proteins. The three prominent bands on the streptavidin-probed blot correspond to the endogenous biotinylated proteins pyruvate carboxylase, propionyl CoA carboxylase, and acetyl-CoA carboxylase. (**D**) Immunofluorescence of individual immortalized *NF2*$^{-/-}$ Schwann cells expressing the BirA constructs and stained for biotin (green) and BirA (red) in the context of an unlabeled confluent monolayer. Scale bar, 10 μm.

The Merlin-$BirA^{R118G}$ fusion colocalized with biotin in transfected Schwann cells (fig. S2A), retained Merlin function by suppressing YAP activity (fig. S2B), and coimmunoprecipitated biotinylated endogenous proteins (fig. S2, C and D). The Dox-inducible cell lines expressed the BirA fusion proteins in roughly equivalent amounts (Fig. 1, B and C), and the subcellular localization of the different fusion proteins was comparable (Fig. 1D). Experiments were performed in confluent cultures, conditions under which Merlin acts as a tumor suppressor. Affinity-purified biotinylated proteins were isolated and identified by mass spectrometry (MS) (fig. S2, F and G). Proteins represented by at least five peptides and increased at least twofold compared to the negative control were considered Merlin proximal (table S1).

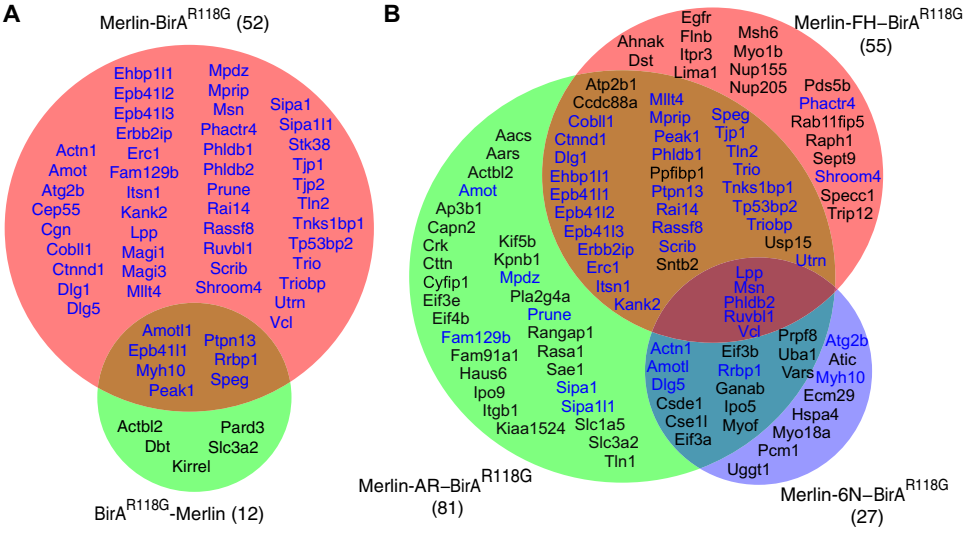

Fig. 2. Proteins biotinylated by Merlin-BirA^{R118G}. (**A**) Venn diagram showing the 52 proteins from cells expressing Merlin-BirA^{R118G} (pink) and the 12 proteins from cells expressing BirA^{R118G}-Merlin (green) that met the selection criteria for Merlin interaction by proximity biotinylation followed by mass spectroscopy. (**B**) Venn diagram showing the 55 proteins from cells expressing Merlin-FH–BirA^{R118G}, 81 proteins from cells expressing Merlin-AR-BirA^{R118G}, and 27 proteins from cells expressing Merlin-6N–BirA^{R118G} that met the selection criteria for Merlin interaction by proximity biotinylation followed by mass spectroscopy. Proteins shown in blue were also identified in the Merlin-BirA^{R118G} dataset in (A).

We identified 52 proteins that were biotinylated in Merlin-BirA^{R118G} cells but not in BirA^{R118G}–A-fos cells (Fig. 2A and Table 1). The most commonly identified peptides mapped to Merlin itself (Table 1, in bold). In addition, we identified the known Merlin-binding proteins Angiomotin (Amot), Angiomotin-like protein 1 (Amotl1) (*37*), the Erbb2-interacting protein Erbb2ip (also known as Erbin) (*53*, *54*), and moesin, validating the specificity of the technique (Table 1, in bold). Peptides from other Merlin-binding proteins, YAP1, Lats1, and Lats2, were detected but did not meet the selection criteria (data file S1), possibly because of a short half-life or not having enough exposed lysines within range of BirA for efficient biotinylation. In contrast, proximity biotinylation using BirA^{R118G}-Merlin identified only 12 proteins, 7 of which were shared with Merlin-BirA^{R118G} (Fig. 2A and Table 1), suggesting that N-terminal BirA^{R118G} may inhibit interactions with Merlin due to steric hinderance.

The PIP_2 binding–deficient mutant, Merlin-6N–BirA^{R118G}, identified a total of 27 proteins, 11 of which were shared with Merlin-BirA^{R118G} (blue text in Fig. 2B and Table 1), thus identifying a set of 41 proteins biotinylated by wild-type Merlin but not by the 6N mutant. The Merlin-FH–BirA^{R118G} mutant identified 55 proteins, 34 of which were also identified by wild-type Merlin-BirA^{R118G} (blue text in Fig. 2B and Table 1). The 21 Merlin-FH–BirA^{R118G} proximal proteins that were not biotinylated by Merlin-BirA^{R118G} define a subgroup of proteins that either require an open conformation to associate with Merlin or interact with Merlin through the CTD. The Merlin-AR–BirA^{R118G} mutant identified 81 proteins, including 42 of the 52 wild-type Merlin-proximal proteins (Fig. 2B and Table 1) and 24 that were unique to the AR mutant, identifying potential binding partners specific for the closed conformation. Note that the proximity biotinylation technique is biased toward high–molecular weight proteins because they have more potential biotinylation sites per molecule than smaller proteins. This bias is reflected in our data, which identified proteins with a median molecular weight of 136 kDa (Table 1), indicating that there are likely low–molecular weight Merlin-proximal proteins that remain unidentified.

Merlin associates with cell junction proteins

Gene ontogeny (GO) analysis indicated that 34 of the 52 proteins proximal to wild-type Merlin fell into three partially overlapping classes of proteins: 30 cell junction proteins, 16 actin-binding proteins, and 11 members of the Hippo pathway (Fig. 3A). Nine of the 11 Hippo pathway proteins are also described as cell junctional components (*44*–*46*), and 14 of the 16 actin-binding proteins are associated with cell junctions (Fig. 3A). Among the 30 cell junction proteins, 19 are associated with adherens junctions, 18 with tight junctions, and 12 with cell-substrate junctions, predominately focal adhesions, with substantial overlap among the classes (Fig. 3B). Nuclear proteins were not enriched in this analysis, consistent with the localization data for Merlin-BirA showing a relative lack of both Merlin-BirA and biotin in the nucleus relative to cell periphery and cytoplasm (Fig. 1C).

We cross-referenced our list of Merlin-proximal proteins with those identified in previous proximity biotinylation studies as localizing to adherens junctions, focal adhesions or tight junctions, or with components of the Hippo pathway (Fig. 3C). These previously published datasets were generated by BirA^{R118G} fusions with the focal adhesion proteins kindlin-2 and paxillin in U2OS osteosarcoma cells (*55*), the adherens junction protein E-cadherin in Madin-Darby canine kidney (MDCK) cells (*56*), the tight junction protein ZO-1 in MDCK cells (*57*), and the Hippo core kinases Lats1 and Lats2 in HeLa and human embryonic kidney (HEK) 293T cells (*46*). Merlin was identified in the kindlin-2, paxillin, Lats1, and Lats2 datasets (*46*, *55*). We found that 28 of 52 Merlin-proximal proteins were also identified in focal adhesion datasets, 25 by kindlin-2–BirA^{R118G} and 22 by paxillin-BirA^{R118G}. The Lats1 and Lats2 datasets shared 18 proteins with our Merlin-BirA^{R118G} dataset, further confirming these associations (*55*). Merlin was not reported in either the E-cadherin or ZO-1 datasets (*56*, *57*). However, 11 merlin-proximal proteins from our data were present in the E-cadherin dataset, and 16 were in the ZO-1 dataset (Fig. 3C). Four Merlin-proximal proteins were common to focal adhesions, adherens junctions, and tight junctions: Scrib, Lpp, Cttnd1, and Erbb2ip. A set of five proteins, Msn, Ruvb1, Vcn, Tln2, and Actn1, were common to tight and adherens junctions. Three proteins were shared by focal adhesions and adherens junctions: Erc1 (ELKS/Rab6-interacting/CAST family member 1), Peak1 (inactive tyrosine-protein kinase PEAK1), and Phactr4 (phosphatase and actin regulator 4). Last, a set of four proteins, Tjp2 (ZO-2), Mllt4 (afadin), Utrn (utrophin), and Tp53bp2 [also called apoptosis-stimulated p53 protein 2 (ASPP2)], was present in the Lats1 and Lats2, focal adhesions, and tight junctions datasets. Overall, 11 proteins have actin-binding activity, as defined by GO analysis (Fig. 3C), suggesting that Merlin may function at the interface between cell adhesion complexes and the actin cytoskeleton. The identification

Table 1. Merlin-proximal proteins. The proteins that met the selection criteria from proximity biotinylation assays with Merlin-BirA^{R118G} are arranged by the average number of MS peptide reads normalized to protein molecular weight, along with the number of peptides from these proteins identified in all other samples. $n = 3$ independent experiments. Merlin and known Merlin-binding proteins Angiomotin (Amot), angiomotin-like protein 1 (Amotl1), Erbin (Erbb2ip), and moesin (Msn) are highlighted in bold.

Gene	Description	MW	Ctrl	WT	BM	FH	AR	6N
Nf2	**Neurofibromin 2 (Merlin)**	69,776	**4.7**	**187.3**	**81.6**	**220.8**	**241.7**	**124.7**
Rai14	Retinoic acid induced 14	108,852	11.2	80	19.2	49.3	61	26.3
Epb41l2	Erythrocyte membrane protein band 4.1-like 2	109,940	10.9	48.7	18.5	81	54.7	19.4
Utrn	Utrophin	392,706	13.9	101.5	12.1	137.8	100	23.7
Mllt4	Afadin	206,499	1.9	48.3	5.9	48.1	29.3	6.8
Amotl1	**Angiomotin-like protein 1**	107,950	**0.6**	**24.4**	**9.1**	**3.6**	**26.9**	**8.5**
Ruvbl1	RuvB-like AAA ATPase 1	50,214	2.2	11.2	1	9	14.6	14
Kank2	KN motif and ankyrin repeat domains 2	90,245	4.4	19.6	3.5	21.2	16.6	9.1
Epb41l3	Erythrocyte membrane protein band 4.1-like 3	103,338	2.8	20.3	5.4	33.3	29.4	7.9
Epb41l1	Erythrocyte membrane protein band 4.1-like 1	98,315	0	19.3	7.3	18.7	14.6	2.2
Tjp1	ZO-1, tight junction protein 1	194,742	3.4	37.3	6.5	21.4	26	5.1
Tp53bp2	ASPP2, tumor protein p53 binding protein 2	125,301	1.8	21.5	0.4	13.3	17.8	2.9
Rassf8	Ras association domain family member 8	48,103	0	8.2	0.8	5.8	9.9	1.7
Vcl	Vinculin	116,717	1.2	17.1	1.2	6.5	16.9	8
Prune	Prune exopolyphosphatase	50,239	0	7	1.7	2.4	6.4	2.9
Mprip	Myosin phosphatase Rho-interacting protein	116,408	2.5	16.2	2.4	24.4	22.8	5
Erc1	ELKS/RAB6-interacting/CAST family member 1	128,331	3.1	17.8	1.7	14.2	26	10.3
Amot	**Angiomotin**	120,915	**0**	**16.2**	**2**	**0**	**14.4**	**4.3**
Phldb2	Pleckstrin homology-like domain, family B member 2	141,486	1.3	18.9	3.4	12.2	14	8.1
Dlg5	Discs, large homolog 5	214,386	0	28.5	0	5	26.9	6.4
Erbb2ip	**Erbb2-interacting protein**	157,248	**0**	**19.3**	**3.4**	**23.6**	**14.9**	**0.5**
Myh10	Myosin heavy chain 10, nonmuscle	228,996	7.5	25.6	43.4	9.9	21.1	35
Lpp	Lipoma-preferred partner	65,891	1	7.1	2.1	6.1	11.7	6.6
Cobll1	Cordon-bleu WH2 repeat protein-like 1	137,382	0.6	14.8	0.4	23.7	8.9	1.6
Stk38	Serine/threonine kinase 38	54,174	0.3	5.7	1.1	4.5	4.4	3.9
Msn	**Moesin**	54,174	**0**	**5.7**	**3.5**	**7.9**	**15.2**	**6.5**
Cep55	Centrosomal protein of 55 kDa	53,930	0	5.3	0.2	0	1.8	0
Actn1	Actinin, α1	103,068	0	10.1	4.3	0.4	12	5.2
Scrib	Scribbled planar cell polarity protein	174,059	0.6	16.4	2.5	15.6	16.7	3.8
Dlg1	Discs, large homolog 1	100,120	0	9.3	1.5	8.6	12.8	0
Phldb1	Pleckstrin homology-like domain, family B, member 1	150,070	0.6	13.8	1.2	18.3	11.3	1.4
Shroom4	Shroom family member 4	163,238	1.8	14.8	1.2	19.3	8.6	2.1
Ptpn13	Protein tyrosine phosphatase, type 13	270,334	1.3	24.4	7.8	23.8	22	5.1
Mpdz	Multiple PDZ domain protein	218,711	0	19.2	0.7	2.4	19.6	2.7
Tnks1bp1	Tankyrase 1 binding protein 1, 182 kDa	181,825	1.5	14.9	2.6	31.3	19.8	7
Tjp2	Tight junction protein 2	131,280	0.3	10.6	1.2	4	3.9	3.2
Phactr4	Phosphatase and actin regulator 4	76,632	0	5.8	0.6	6.1	4	0.5
Fam129b	Family with sequence similarity 129, member B	84,819	0	6	3.7	2.6	6	2.5
Ctnnd1	Catenin (cadherin-associated protein), δ1	104,925	0	7.3	1.6	5.8	5.3	1.4
Peak1	Pseudopodium-enriched atypical kinase 1	191,097	0.6	12.7	5.6	17.4	13.1	4.8
Tln2	Talin 2	253,621	0.3	15.1	0	7.6	8.3	0.5
Triobp	TRIO and F-actin binding protein	223,368	0.9	13.2	2	16.4	11.6	1.6

continued on next page

Gene	Description	MW	Ctrl	WT	BM	FH	AR	6N
Sipa1	Signal-induced proliferation-associated 1	112,066	0.6	6	0.4	4.5	8	3.5
Sipa1l1	Signal-induced proliferation-associated 1-like 1	197,031	0	9.9	1.9	4.1	6	0.9
Magi3	Membrane associated guanylate kinase 3	161,672	0	6.7	2.3	0	3.5	0
Ehbp1l1	EH domain binding protein 1-like 1	184,834	0	7.4	0	19.9	7.8	1.6
Cgn	Cingulin	136,447	0	5.3	0	0	2.3	0
Rrbp1	Ribosome binding protein 1	172,879	0.6	5.7	11.7	2.2	10.1	5.8
Magi1	Membrane associated guanylate kinase 1	161,974	0	5.3	3.8	1.6	2	0
Atg2b	Autophagy-related 2B	231,399	0	7.1	1.4	2.4	3.5	5.5
Itsn1	Intersectin 1	194,297	0	5.6	0	8.5	5.1	0
Speg	SPEG complex locus	354,343	0.9	8.7	19.1	11.2	13.4	1
Trio	Trio Rho guanine nucleotide exchange factor	347,861	0.6	6.3	1.4	9.6	5	0.7

of Merlin-proximal proteins as components of cell junctions suggests an integral role for Merlin in signal transduction from these complexes.

Merlin coimmunoprecipitates with some of the proteins identified by proximity biotinylation

Proximity biotinylation does not distinguish between direct binding versus indirect interaction through a complex or close proximity. We therefore designed a secondary screen in which bait proteins fused to red fluorescent protein (RFP) were cotransfected into HEK 293T cells with a probe consisting of Merlin fused to NanoLuc (NLuc) (*58*), a small, bright luciferase with low nonspecific binding activity (fig. S3A). RFP was pulled down by a high-affinity, nanobody-based RFP-binding protein covalently bound to magnetic beads (Fig. 4A). The fraction of luciferase activity bound to beads, normalized to the amount of RFP fluorescence on the beads, and provides a sensitive and quantitative assay for Merlin interaction. We cloned a representative set of 10 complementary DNAs encoding Merlin-proximal proteins in frame with RFP: Angiomotin (Amot), α-actinin (Actn1), afadin (Mltt4), ASPP2 (Tp53bp2), band 4.1B (Epb41l2), myosin IIB (Myh10), Rassf8 (Rassf8), Scribble (Scrib), vinculin (Vcn), and ZO-1 (Tjp1). We included Lats1, another known Merlin-binding protein, as an additional positive control and RFP alone as a negative control.

Cotransfection experiments in HEK 293T cells confirmed complex formation with Merlin for 7 of 10 proteins tested: Angiomotin α-actinin, afadin, ASPP2, Lats1, myosin IIB, Scrib, and ZO-1. Angiomotin interacted with the highest apparent affinity (~100-fold greater than the negative control), ASPP2 and Lats1 interacted more than 20-fold over control, and the remaining proteins (α-actinin, afadin, band 4.1B, Scrib, and ZO-1) all bound Merlin two- to fivefold over control. Band 4.1B, myosin IIB, and vinculin were negative in this assay (Fig. 4B), suggesting that these proteins are proximal to Merlin rather than present in a complex with Merlin interacting or that cell type differences are responsible for this result.

ASPP2 directly binds to Merlin

To test for direct binding to Merlin, we performed immunoaffinity purification of the RFP-fused proteins from transfected HEK 293T cell lysates using a magnetic bead–conjugated nanobody recognizing RFP. This generated RFP fusion proteins, purified to near homogeneity, bound to magnetic beads (fig. S3B). We tested for direct interactions by incubating RFP bait protein–bound beads with purified Merlin-NLuc fusion proteins (fig. S3, C and D), then washing and measuring luciferase activity. Merlin bound directly to 3 of the 11 proteins we tested: the known Merlin-interacting proteins Angiomotin and Lats1, as well as ASPP2. Angiomotin bound most effectively, 2300-fold greater than the negative control, again suggesting a high-affinity interaction (Fig. 4C). ASPP2 and Lats1 bound 125- and 268-fold above control, respectively (Fig. 4C). The remaining tested proteins did not bind directly to Merlin-NLuc under these conditions. These experiments identify ASPP2, a proapoptotic transcriptional coactivator localized to both cell junctions and the nucleus (*59*), as a previously unknown Merlin-binding protein. ASPP2 bound to wild-type Merlin with a greater apparent affinity than to Merlin-FH, Merlin-AR, or Merlin-6N (Fig. 4D), correlating with the MS data for these mutant forms of Merlin (Table 1). In addition, ASPP2 binding to the phosphorylation site mutant S518A was nearly twofold greater than to wild-type Merlin, whereas ASPP2 binding to the phosphomimetic mutant S518D was more than twofold less than wild-type, suggesting that ASPP2 interacts specifically with hypophosphorylated Merlin (Fig. 4D). ASPP2 binding was also impaired in the patient-derived mutations Δ39-121, L360P, and ΔN18, the last of which is a deletion of the first 18 amino acids (Fig. 4D) (*21*, *60*).

The N terminus of ASPP2 binds to the FERM domain of Merlin in the closed conformation

To map the Merlin-binding domains of ASPP2, we generated a series of RFP-ASPP2 deletion mutants (Fig. 5A) and tested these for binding to purified Merlin-NLuc in vitro. We found that Merlin bound to sequences between amino acids 125 and 335 in the N-terminal half of ASPP2 (Fig. 5A). To determine which Merlin domains were responsible for ASPP2 binding, we performed binding experiments using Merlin deletion mutants. These included a CTD deletion mutant in which the FERM and helical domains were intact (Merlin-FH–NLuc), an N-terminal truncation missing the FERM domain but retaining the helical and CTD domains (Merlin-HC–NLuc), and a dual CTD and FERM truncation containing only the central helical region (Merlin-H–NLuc). As controls, we tested binding of Angiomotin and Lats1 to these deletion mutants (Fig. 5B). As expected, Angiomotin bound to full-length Merlin most efficiently, bound to Merlin-HC less efficiently, but did not bind to Merlin-FH or to the helix alone (Fig. 5B). Lats1 preferentially bound to Merlin-FH relative to full-length but not to Merlin-HC or Merlin-H (Fig. 5B). ASPP2 bound

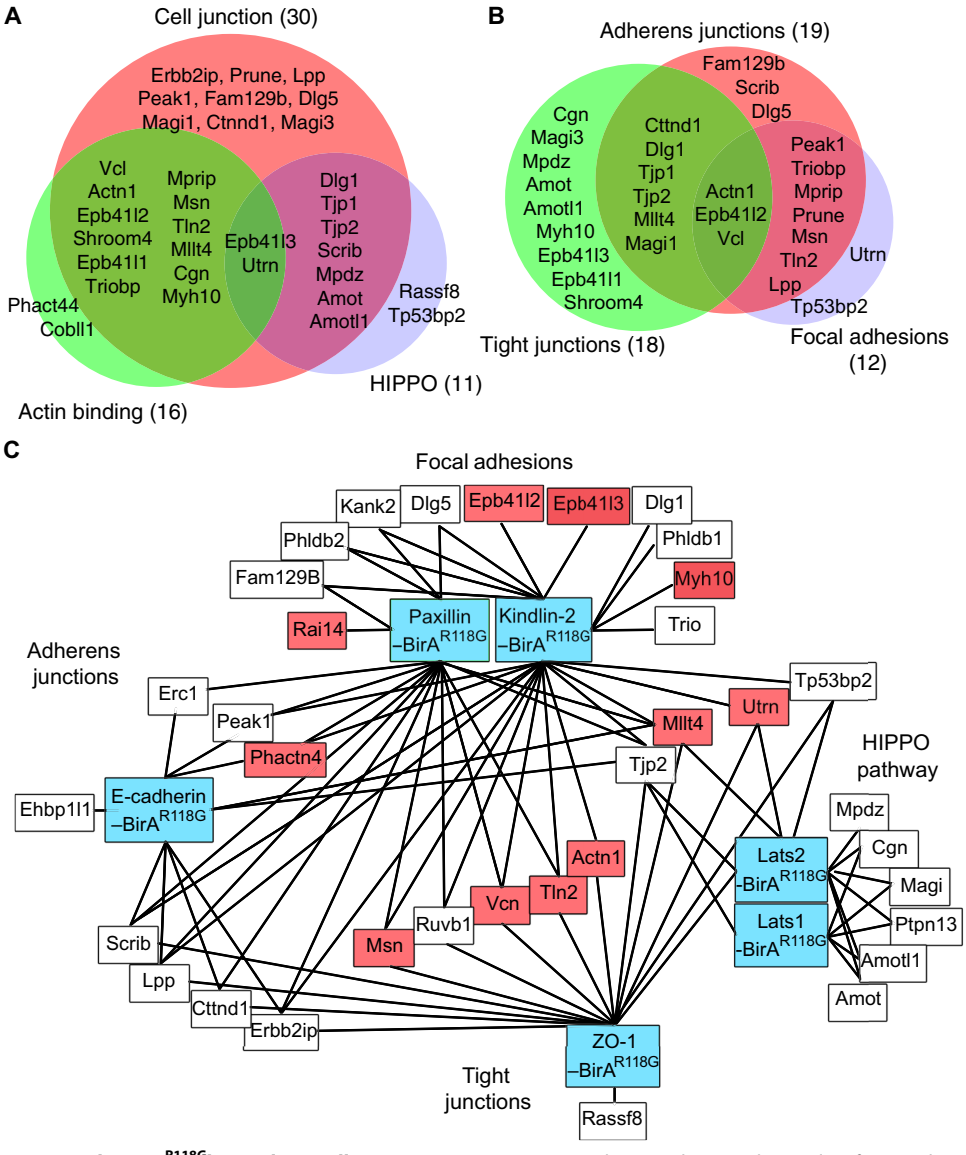

Fig. 3. Merlin-BirA^{R118G}biotinylates cell junction proteins. (**A**) Venn diagram showing the results of GO analysis performed on Merlin-associated proteins identified by proximity biotinylation mass spectroscopy that are components of cell junctions, bind to actin, or are members of the Hippo pathway. (**B**) Venn diagram of Merlin-associated cell junction proteins that are components of adherens junctions, tight junctions, and focal adhesions, based on GO analysis. (**C**) Proximity map of proteins biotinylated by Merlin-BirA^{R118G} connected by lines to previously published proximity biotinylation datasets (blue boxes) generated for focal adhesions [Kindlin-2–BirA^{R118G} and Paxillin-BirA^{R118G} (*55*)], tight junctions [ZO-1–BirA^{R118G} and BirA^{R118G}–ZO-1 (*57*)], adherens junctions [E-cadherin– BirA^{R118G} (*56*)], and the Hippo pathway [Lats1 and Lats2 (*46*)]. Actin-binding proteins are highlighted in pink (*55*).

most efficiently to full-length Merlin, showed reduced interaction with Merlin-FH, and did not bind to the Merlin-HC or Merlin-H (Fig. 5B). These data suggest that ASPP2 binds to the FERM domain when Merlin is in a closed conformation, whereas Lats binds to regions of the FERM domain that are masked by the CTD in the closed conformation, and Angiomotin binds to the CTD (*13*). Both Angiomotin and ASPP2 bind most effectively to full-length Merlin but interact through distinct binding sites (Fig. 5B), suggesting that both might bind Merlin simultaneously. However, cotransfection of HEK 293T cells Merlin with RFP-Angiomotin and green fluorescent protein (GFP)–tagged ASPP2 showed that RFP-Angiomotin coprecipitated with Merlin but not with GFP-ASPP2 (Fig. 5C). This suggests that distinct Merlin conformations are required to bind to ASPP2, Angiomotin, and Lats1 (Fig. 5D).

DISCUSSION

There has been a great deal of progress in bringing Merlin function into focus. Experiments in *Drosophila melanogaster* demonstrated that Merlin activates the Hippo pathway (*42*, *61*–*63*), leading to the observation that Merlin binds to and activates the core Hippo kinase Lats (*43*), delineating a biochemical mechanism that links Merlin to a specific signal transduction cascade that is consistent with the genetic phenotypes observed in the fly. Concurrently, the realization that PIP_2 binding is required for Merlin localization and activity (*18*, *19*) reinforced the view that lipid rafts at the intracellular face of the plasma membrane are a critical locus of tumor suppressor function, an observation that is consistent with a role in the Hippo pathway and with our data placing Merlin in cell junctional complexes. Additional studies have also yielded a clearer view of the conformational changes that Merlin undergoes to perform its functions (*12*, *52*), including the discovery that Angiomotin binding (*13*) and PIP_2 interaction (*14*) induce conformational changes that increase the accessibility of the FERM domain. Experiments identifying Angiomotin as a key Merlin-binding protein further link Merlin to cell junctional proteins, Merlin's known regulation of Rac activity (*37*), and the Hippo pathway (*64*). However, despite these advances, the full scope of Merlin activity remains unclear.

We used proximity biotinylation combined with mass spectroscopy to define a cohort of proteins that associate with Merlin in confluent, living Schwann cells. Because biotinylation occurs within live cells under normal physiological conditions, low-affinity interactions may be detected (*65*, *66*). We identified a set of Merlin-proximal proteins that defines the molecular environment in which Merlin functions and defined a comprehensive list of possible binding partners through which it acts, representing a global perspective on Merlin function. Most Merlin-proximal proteins in this dataset are components of either cell-cell or cell–extracellular matrix junctions, including cadherin-based adherens junctions, claudin-based tight junctions, integrin-based focal adhesion complexes, the polarity complex, and the laminin-binding dystrophin glycoprotein complex (*67*). These data are consistent with Merlin localization to the

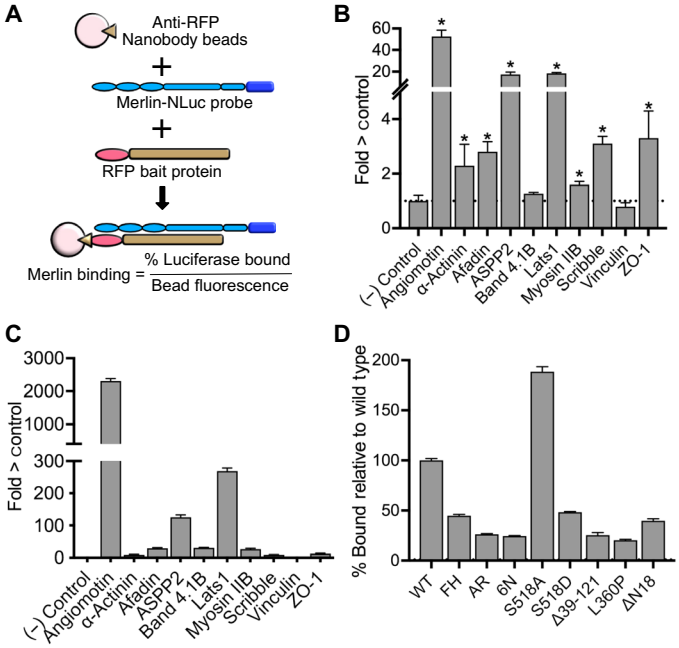

Fig. 4. Indirect and direct Merlin binding assays. (**A**) Schematic diagram of the basic RFP pull-down assay with extracts of HEK 293T cells coexpressing RFP fused to bait proteins and a Merlin-Nanoluciferase probe (Merlin-NLuc) immunoprecipitated using a nanobody directed against RFP bound to magnetic beads. Data are expressed as % luciferase activity bound and normalized to red fluorescence on the bead (excitation 565 nm, emission 590). (**B**) Indirect interaction assays showing the relative luciferase activity that coimmunoprecipitated with the indicated RFP-tagged bait proteins from HEK 293T cells coexpressing the bait and Merlin-NLuc. RFP alone (no bait) was a negative control, and RFP-Angiomotin was a positive control. The dotted line represents the luciferase activity in the RFP-only negative control. Data are means relative to control ± SD; $n = 3$ independent experiments. *$P > 0.05$ by Student's t test relative to control. (**C**) Direct binding assays showing the luciferase activity bound to purified RFP bait proteins that had been incubated with purified Merlin-NLuc. The dotted line represents the luciferase activity in the RFP-only negative control. Representative data of $n > 3$ independent biological experiments relative to control. (**D**) Relative binding of ASPP2 to the Merlin mutants used in the proximity biotinylation experiments (Merlin-FH, Merlin-AR, and Merlin-6N), the phosphorylation-deficient mutant S518A, the phosphomemetic mutant S518A, patient-derived mutations Δ39-121 and L360P, and the 18–amino acid N-terminal deletion mutant ΔN18. The dotted line represents the luciferase activity with wild-type (WT) Merlin. Data are means relative to wild type ± SD; $n = 3$ biological replicates.

cell periphery (*68*, *69*) and the observation that Merlin is critical for the organization of Schwann cell contacts in peripheral nerves (*16*).

The ability of wild-type and mutant forms of Merlin to biotinylate nearby proteins also provides insight into Merlin structure and function. $BirA^{R118G}$-Merlin, in which $BirA^{R118G}$ is fused to the N terminus of Merlin, was much less efficient at biotinylating proximal proteins, suggesting a critical role for the Merlin N terminus that is blocked by the BirA fusion. This result is supported by the impaired binding of ASPP2 to the ΔN18 Merlin mutant, which is missing the first 18 amino acids, a region required for localization to the cell periphery (*21*). Reduced biotinylation and impaired ASPP2 binding by the PIP_2 binding mutant, Merlin-6N, (*19*), is consistent with a critical function for PIP_2 in Merlin localization and conformation (*14*, *19*). It is also in line with the key role that PIP_2 plays in both adherens junction and focal adhesion signaling (*70*–*74*).

Two mutant Merlin proteins, Merlin-FH and Merlin-AR, provided insight into Merlin interactions that are conformation dependent. Because the current model for Merlin function holds that the CTD functions as a gate that toggles between open, FERM-accessible and closed, FERM-inaccessible conformations, we reasoned that deletion of the CTD would identify proteins that bind to an open, FERM-accessible conformation. The AR mutant has a more stable FERM-CTD interaction (*52*) and was predicted to favor proteins that are specific for the closed conformation. Our initial assumption was that the open-conformation mutant Merlin-FH would biotinylate more proteins by virtue of its increased access to the FERM domain. We presumed that the closed conformation mutant Merlin-AR would biotinylate fewer proteins because of reduced access to the FERM domain. However, our results were not consistent either of with these assumptions. We did not find a substantial increase in proteins biotinylated by the open-conformation mutant, Merlin-FH, as would be expected if the CTD functioned to block access to the FERM domain, although subsequent binding studies with Lats are consistent with this model. Compared to wild-type Merlin, Merlin-FH failed to biotinylate 20 proteins, including both Angiomotin and Amotl1, proteins that had previously been shown to interact with Merlin through the CTD (*13*, *37*). We now view the Merlin-FH mutant as predominately identifying proteins that require the CTD to interact, rather than those specific for an open conformation. In contrast, Merlin-AR biotinylated a greater number of proteins than did wild-type Merlin, opposite to what would be expected if the closed conformation resulted in inaccessible binding sites. Instead, these results identified a large cohort of Merlin-associated proteins that are specific for the closed conformation, suggesting a possible distinct function for this conformation. Proteins biotinylated by Merlin-AR overlapped with those biotinylated by Merlin-6N, suggesting that the PIP_2 binding–deficient Merlin-6N mutant also exists in a closed conformation. This supposition is consistent with recent structural studies showing that the Merlin FERM-CTD domain interaction is reduced upon PIP_2 binding, showing that non–PIP_2-bound Merlin exists in a closed conformation (*14*).

We identified ASPP2 as a direct binding partner for Merlin. ASPP2 was originally identified as a p53 binding protein (*75*) that enhances p53 DNA binding and transcriptional activity on proapototic promoters (*76*), hence the gene name *Tp53bp2*. ASPP2 is a haploinsufficient tumor suppressor (*77*) that also interacts with a host of oncogenes and tumor suppressors, including Ras, nuclear factor κB, YAP, and members of the Bcl family (*59*, *78*–*80*). Merlin binds to ASPP2 between amino acids 125 and 335, a putative α-helical, glutamine-rich region reminiscent of transcriptional transactivation domains (*81*). Our evidence that ASPP2 binding to phosphorylated Merlin is impaired suggests that phosphorylation at Ser^{518}, mediated by PAK1 (p21 activating kinase 1) (*82*), is a point of regulation of the Merlin-ASPP2 interaction. Our data suggest that ASPP2 binds to Merlin when Merlin is in a closed conformation, mainly through the FERM domain, stabilized by sequences in the CTD. This binding conformation is distinct from that bound by Angiomotin, which binds to and interacts with the CTD or Lats, which binds to FERM domain regions that are masked by the CTD (*13*). These data suggest that there are multiple combinations of conformations and binding sites for Merlin partners that imply more subtle and complex functions than the simple open and closed conformations described by current models.

Cell junctions are multiprotein complexes responsible for cell-cell and cell-substrate interactions that perform anchoring and barrier

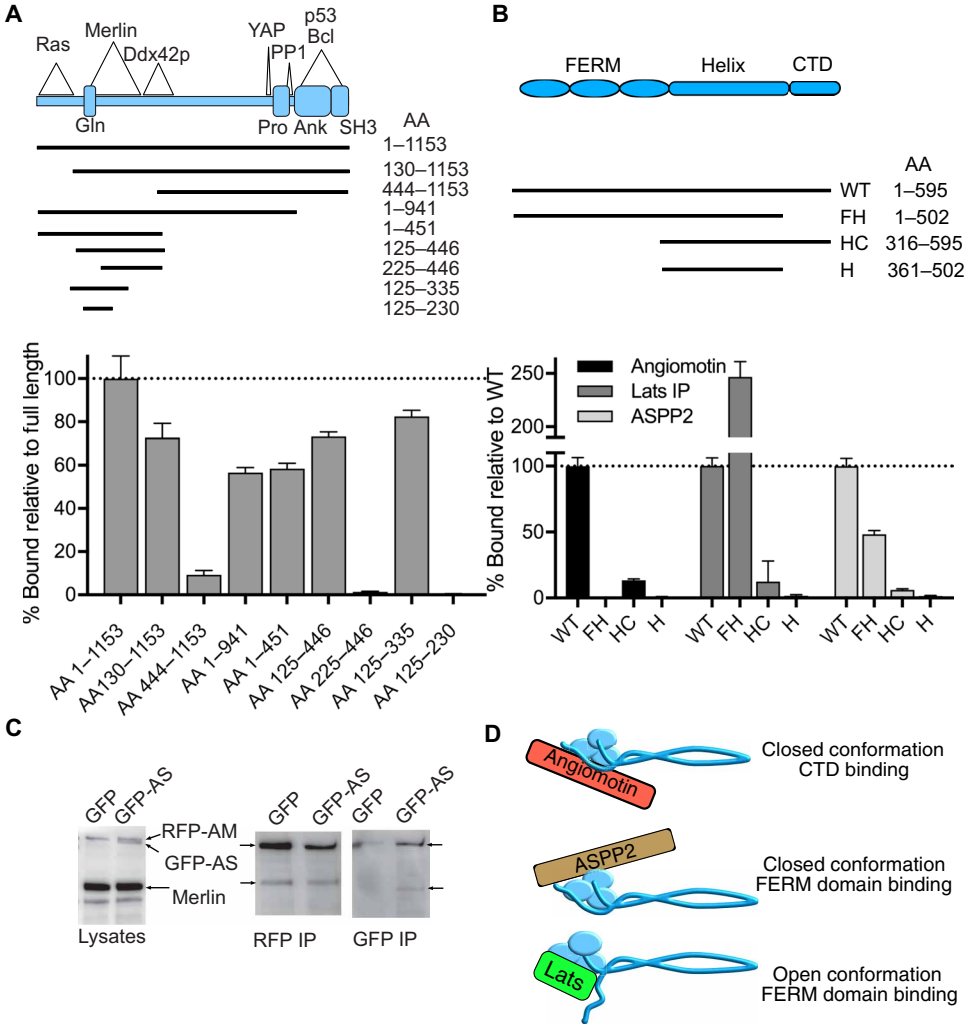

Fig. 5. ASPP2-Merlin binding. (**A**) Schematic diagram of ASPP2 deletion mutants used to map the Merlin-binding domain. The regions of known interactions with Ras, Merlin, Ddx42p, YAP, PP1, p53, and Bcl and the known structural domains are noted in the diagram. Gln, Gln-rich domain; Pro, proline-rich domain; Ank, ankyrin repeat region; SH3, SH3 domain; AA, amino acid. Quantification of Merlin-NLuc binding to RFP-ASPP2 deletion mutants using purified proteins. Data are means relative to full-length ASPP2 ± SD; $n = 3$ biological replicates. (**B**) Schematic diagram of the domain structure of Merlin and the Merlin-NLuc deletion mutants used to map ASPP2-binding regions. WT, full-length wild-type; FH, FERM-helix (CTD deleted); HC, helix-CTD (FERM deleted); H, helix (CTD and FERM deleted). Quantification of Merlin-NLuc deletion mutants binding to RFP-Angiomotin, RFP-Lats1, and RFP-ASPP2 using purified proteins; $n = 3$ biological replicates. (**C**) Lysates of HEK 293T cells cotransfected with Merlin-NLuc and RFP-angiomotin (RFP-AM) and either GFP alone or GFP-ASPP2 (GFP-AS) were subjected to Western blotting, RFP immunoprecipitation (RFP IP), or GFP immunoprecipitation (GFP IP) and probed with a combination of antibodies directed against Merlin, GFP, and RFP. (**D**) Schematic diagram depicting the proposed protein-protein interactions of different Merlin conformations. We propose that Angiomotin binds to the closed conformation of Merlin at the CTD, ASPP2 binds to the closed conformation of Merlin through the FERM domain, and Lats1 binds to the open conformation of Merlin through the FERM domain.

functions that are critical for mechanical stability and tissue homeostasis and are frequently disrupted in neoplastic cells (*83*–*86*). They are also components of mechanosensory signal transduction pathways that mediate cellular responses to external mechanical forces and integrate these signals with growth regulation (*87*). Our data are consistent with findings suggesting that Merlin plays a role in mechanosensing at cell junctions (*88*, *89*) and greatly expands the scope of Merlin function by identifying multiple potential interaction partners in adherens junctions, tight junctions, and focal adhesion, all of which participate in mechanotransduction (*90*). Merlin's role in regulating the Hippo pathway (*42*), an explicit mechanosensory signaling system (*91*), and its interaction with junctional signaling proteins such as Angiomotin, Lats1, and YAP1 (*92*) highlight this activity. Merlin is necessary for nucleocytoplasmic shuttling of YAP1 (*39*) and mediates the export of YAP1 from the nucleus in response to changes in the adhesion status of β1 integrin (*93*) or actin-myosin II–generated mechanical tension in circumferential actin belts (*94*). It is possible that the lack of nuclear proteins in our datasets reflects Merlin's transient residence in the nucleus due to its function as a nucleocytoplasmic shuttling factor. Many of the cell junction proteins identified in our experiments have also been described as nuclear proteins. These include afadin, ZO-1, RAI14, and ASPP2 (*95*–*98*), suggesting that Merlin may mediate the nucleocytoplasmic shuttling of these and other cell junctional proteins as it does for YAP (*93*). Merlin has been shown to inhibit the function of focal adhesion kinase 1 (FAK1) (*99*), a cell junctional signaling molecule that is directly responsive to mechanical stress in integrin-based cell adhesion complexes (*100*–*104*). The clinical effectiveness of FAK1 inhibitors inversely correlates with Merlin abundance in ovarian cancer and mesothelioma (*105*, *106*), thereby linking Merlin with a mechanosensory pathway that may be an attractive therapeutic target in schwannoma. Going forward, the challenge will be to use this information to fully understand Merlin's tumor suppressor function in order to devise new strategies to treat NF2.

MATERIALS AND METHODS

Cell lines

HEK 293T and immortalized mouse $Nf2^{flox2/flox2}$ Schwann cells, a gift from D. Lallemand (Centre National de la Recherche Scientifique, Institut Curie, Paris, France) (*22*), were maintained in Dulbecco's minimum essential medium, 10% fetal bovine serum, and PenStrep (Life Technologies) at 37°C, 95% humidity, and 7.5% CO_2. Merlin-null cells were generated by infecting $Nf2^{flox2/flox2}$ Schwann cells with adenovirus expressing Cre recombinase (Kerafast). All cell lines were routinely tested for mycoplasma contamination.

Antibodies and reagents

Horseradish peroxidase (HRP) conjugated an antibody specific for GFP (cat. no. 600-103-215) was from Rockland and specific for RFP (cat no. ab34767) was from Abcam. Antibody specific for YAP1 was from Cell Signaling Inc. Anti-Merlin monoclonal antibody 4B5 was made by W. Ip (*12*). HRP-conjugated secondary antibodies were from Jackson ImmunoResearch Laboratories. Strep-Tactin resin was from (IBA Lifesciences).

Plasmids

mApple-N1 (Addgene plasmid no. 54567) was a gift from M. Davidson. pSK ZO-1 (Addgene plasmid no. 30316) was a gift from J. Anderson and A. Fanning, CMV-GFP-NMHC II-B (Addgene plasmid no. 11348) was a gift from R. Adelstein, pGFP(C3)-vinculin (Addgene plasmid no. 30312) was a gift from K. Hahn, pKvenus-Scrib (Addgene plasmid no. 58738) was a gift from I. Macara, and pEGFP-C3-hYAP1 and pEGFP C3-Lats1 (Addgene plasmid nos. 19053 and 17843, respectively) were gifts from M. Sudol. HA-AMOT p130 (Addgene plasmid no. 32821) was a gift from K. Guan. pcDNA3.1-ccdB-NLuc (Addgene plasmid no. 87067) was a gift from M. Taipale. GFP-afadin was a gift from Y. Takai (*107*). GFP-ASPP2 was a gift from C. D. Lopez (*108*). p4XBS2WT-Luc (Addgene plasmid no. 16593) was a gift from B. Vogelstein. p8xGTIIC-luciferase (Addgene plasmid no. 34615) was a gift from S. Piccolo. pcDNA3 p53 WT (Addgene plasmid no. 69003) was a gift from D. Meek. Plasmids containing the open reading frames for Epb4.1l3 and Rassf8 from the Human ORFeome V1 were purchased from the DNASU Plasmid Repository at the Arizona State University. pRL-TK was purchased from Promega. The Tet-inducible plasmids, pTRE3G-BI-ZsGreen and pCMV-Tet3G, were purchased from Tanaka Holdings.

Cloning

Dox-inducible expression plasmids expressing $BirA^{R118G}$ fusion proteins were generated using standard restriction enzyme–based cloning techniques. Expression vectors for RFP, GFP, and luciferase were fused to StrepTag II in-frame either N-terminal or C-terminal to the RFP, GFP, or NLuc to facilitate affinity purification. Plasmids expressing test proteins and Merlin probes were assembled from high-fidelity polymerase chain reaction–amplified fragments (Tanaka Holdings) using Gibson assembly (InFusion, Tanaka Holdings). All cloning operations were confirmed by sequencing.

Mass spectrometry

Dox-inducible cell populations were generated by cotransfecting the pTRE3G-inducible expression plasmid with the pCMV-Tet3G regulatory plasmid into Merlin-null Schwann cells. G418-resistant colonies were pooled, expanded, induced Dox, and sorted for the brightest 10% green fluorescence of the population (Beckman Coulter MoFlo XDP).

Cells were grown to confluence in two Falcon five-tiered flasks (872 cm^2), induced with Dox in the presence of D-biotin, and incubated for 48 hours. Cells were then trypsinized, washed in cold PBS, and pelleted and lysed in 5 ml of radioimmunoprecipitation assay supplemented with a protease inhibitor cocktail (HALT, Pierce) and benzonase (Sigma-Aldrich). Biotinylated proteins were isolated as described by Roux *et al.* (*109*), using 250 µl of streptavidin magnetic beads (Streptavidin Dynabeads, Life Technologies), eluted in 50 µl of 1× Laemmli sample incubated at 95°C for 20 min. Samples were run on a 7.5% SDS–polyacrylamide gel electrophoresis (PAGE) (Bio-Rad), stained with colloidal Coomassie Blue (Life Technologies), excised and sent to the Taplin Biological Mass Spectrometry Facility at Harvard Medical School, and processed for matrix-assisted laser desorption/ionization mass spectroscopy. Mass spectroscopy experiments were performed in triplicate. Peptides that mapped to endogenous biotinylated proteins were used as an internal control to normalize replicates. Simple descriptive statistics were used to evaluate the data. Proteins were considered positive if they averaged at least five mapped peptides and were at least twofold plus an SD above the $BirA^{R118G}$–A-fos–negative control. GO analysis was performed using g:Profiler (*110*). Venn diagrams were generated using BioVenn (*111*). Proximity maps were generated using PathVisio software (*112*).

Interaction assays

HEK 293T cells were cotransfected with RFP-target and Merlin-NLuc plasmids, lysed in 0.5 ml of 20 mM tris-Cl (pH 7.4), 0.15 M NaCl [tris-buffered saline (TBS)] and 2 mM $MgCl_2$, 0.5% NP-40, 1× HALT protease inhibitor mix (Thermo Fisher Scientific, Waltham, MA), and 2.5 U benzonase (Sigma-Aldrich, St. Louis, MO). Lysates were diluted 1:2.5 with TBS (pH 7.4) and 0.05% Tween 20 (TBST), and then, NLuc activity was measured using Nano-Glo reagent (Promega, Madison, WI). RFP or GFP fusion proteins were immunoprecipitated using RFP-Trap_MA or GFP-Trap_MA (ChromoTek, Hauppauge, NY), recovered using a magnetic stand, and washed four times with TBST. The beads were transferred to the wells of a white 96-well plate. NLuc luciferase activity was measured on a FlexStation 3 (Molecular Devices, San Jose, CA). Immunoprecipitation-associated luciferase was normalized to the activity in the lysates. RFP-Trap_MA beads were recovered, rinsed in TBS, resuspended in 1× Instant-Bands loading dye (EZBiolab, Indianapolis, IN), boiled for 10 min, and run on a 4 to 20% tris-glycine SDS-PAGE gel.

Direct binding assays

To purify Merlin-NLuc probes, 5×10^6 HEK 293T cells were plated into each of two 15-cm dishes and then transfected with 50 µg of pMerlin-NLuc-StrepTag plasmid per plate using polyethylenimine (PEI) using a 3:1 PEI-to-DNA ratio. Cells were harvested in 0.5 ml of TBS (pH 7.4), 2 mM $MgCl_2$, 0.1% CHAPS plus HALT protease inhibitor mix (Thermo Fisher Scientific), and 2.5 U benzonase (Sigma-Aldrich), and cleared lysates were concentrated using Amicon-10 spin concentrators. Washed magnetic Strep-Tactin beads (100 µl; MagStrep type3 XT, IBA Life Sciences) were added and incubated overnight at 4°C with agitation. Beads were recovered by magnet, washed three times each with high-salt buffer [20 mM tris-Cl (pH 8.0), 0.5 M NaCl, 1% Triton X-100, and 0.05% Tween 20 and 0.5 mM EDTA], low-salt buffer [20 mM tris-Cl (pH 8.0), 50 mM NaCl, 10% glycerol, 0.5% NP-40, and 0.05% Tween 20 and 0.5 mM EDTA], and an isotonic buffer [20 mM tris-Cl (pH 8.0),150 mM NaCl, and 0.05% Tween 20 and 0.5 mM EDTA], and then eluted in 200 µl of 50 mM D-biotin in TBS. Protein concentration and purity of an aliquot was evaluated by 4 to 20% SDS-PAGE against a standard curve of bovine serum albumin (BSA) stained with Instant-Bands fluorescent total protein stain and visualized on an Azure c600 imaging system.

For small-scale affinity purification, RFP-bait expressing plasmid was transfected into HEK 293T cells, lysed as described above then affinity purified with RFP-Trap_MA beads, washed as described above, and resuspended in TBST. The bead solution was split; half was evaluated for concentration and purity as described

above. The remaining half of the beads was resuspended in a 30-µl reaction mix containing TBST and BSA (0.5 mg/ml) and 30 to 50 nM Merlin-NLuc protein and incubated at room temperature for 1 hour. Then, RFP-Bait bound beads were then recovered, washed four times with TBST, and NLuc luciferase activity was measured as described above.

SUPPLEMENTARY MATERIALS

stke.sciencemag.org/cgi/content/full/12/578/eaau8749/DC1
Fig. S1. Characterization of *Nf2*$^{-/-}$ Schwann cells.
Fig. S2. Validation of proximity biotinylation reagents.
Fig. S3. Merlin-NLuc interaction analysis.
Table S1. All proteins above threshold.
Data file S1. Merlin proximity biotinylation data.

REFERENCES AND NOTES

1. G. A. Rouleau, P. Merel, M. Lutchman, M. Sanson, J. Zucman, C. Marineau, K. Hoang-Xuan, S. Demczuk, C. Desmaze, B. Plougastel, S. M. Pulst, G. Lenoir, E. Bijlsma, R. Fashold, J. Dumanski, P. de Jong, D. Parry, R. Eldrige, A. Aurias, O. Delattre, G. Thomas, Alteration in a new gene encoding a putative membrane-organizing protein causes neuro-fibromatosis type 2. *Nature* **363**, 515–521 (1993).
2. M. MacCollin, T. Mohney, J. Trofatter, W. Wertelecki, V. Ramesh, J. Gusella, DNA diagnosis of neurofibromatosis 2. Altered coding sequence of the merlin tumor suppressor in an extended pedigree. *JAMA* **270**, 2316–2320 (1993).
3. S. Ammoun, C. O. Hanemann, Emerging therapeutic targets in schwannomas and other merlin-deficient tumors. *Nat. Rev. Neurol.* **7**, 392–399 (2011).
4. A. M. Petrilli, C. Fernández-Valle, Role of Merlin/NF2 inactivation in tumor biology. *Oncogene* **35**, 537–548 (2016).
5. M. Giovannini, E. Robanus-Maandag, M. van der Valk, M. Niwa-Kawakita, V. Abramowski, L. Goutebroze, J. M. Woodruff, A. Berns, G. Thomas, Conditional biallelic Nf2 mutation in the mouse promotes manifestations of human neurofibromatosis type 2. *Genes Dev.* **14**, 1617–1630 (2000).
6. J. R. Gehlhausen, S.-J. Park, A. E. Hickox, M. Shew, K. Staser, S. D. Rhodes, K. Menon, J. D. Lajiness, M. Mwanthi, X. Yang, J. Yuan, P. Territo, G. Hutchins, G. Nalepa, F.-C. Yang, S. J. Conway, M. G. Heinz, A. Stemmer-Rachamimov, C. W. Yates, D. Wade Clapp, A murine model of neurofibromatosis type 2 that accurately phenocopies human schwannoma formation. *Hum. Mol. Genet.* **24**, 1–8 (2015).
7. H. Morrison, L. S. Sherman, J. Legg, F. Banine, C. Isacke, C. A. Haipek, D. H. Gutmann, H. Ponta, P. Herrlich, The NF2 tumor suppressor gene product, merlin, mediates contact inhibition of growth through interactions with CD44. *Genes Dev.* **15**, 968–980 (2001).
8. J. A. Trofatter, M. M. MacCollin, J. L. Rutter, J. R. Murrell, M. P. Duyao, D. M. Parry, R. Eldridge, N. Kley, A. G. Menon, K. Pulaski, V. H. Haase, C. M. Ambrose, D. Munroe, C. Bove, J. L. Haines, R. L. Martuza, M. E. MacDonald, B. R. Seizinger, M. P. Short, A. J. Buckler, J. F. Gusella, A novel moesin-, ezrin-, radixin-like gene is a candidate for the neurofibromatosis 2 tumor suppressor. *Cell* **75**, 826 (1993).
9. A. Bretscher, K. Edwards, R. G. Fehon, ERM proteins and merlin: Integrators at the cell cortex. *Nat. Rev. Mol. Cell Biol.* **3**, 586–599 (2002).
10. Q. Li, M. R. Nance, R. Kulikauskas, K. Nyberg, R. Fehon, P. A. Karplus, A. Bretscher, J. J. G. Tesmer, Self-masking in an intact ERM-merlin protein: An active role for the central α-helical domain. *J. Mol. Biol.* **365**, 1446–1459 (2007).
11. R. Nguyen, D. Reczek, A. Bretscher, Hierarchy of merlin and ezrin N- and C-terminal domain interactions in homo- and heterotypic associations and their relationship to binding of scaffolding proteins EBP50 and E3KARP. *J. Biol. Chem.* **276**, 7621–7629 (2001).
12. R. F. Hennigan, L. A. Foster, M. F. Chaiken, T. Mani, M. M. Gomes, A. B. Herr, W. Ip, Fluorescence resonance energy transfer analysis of merlin conformational changes. *Mol. Cell. Biol.* **30**, 54–67 (2010).
13. Y. Li, H. Zhou, F. Li, S. W. Chan, Z. Lin, Z. Wei, Z. Yang, F. Guo, C. J. Lim, W. Xing, Y. Shen, W. Hong, J. Long, M. Zhang, Angiomotin binding-induced activation of Merlin/NF2 in the Hippo pathway. *Cell Res.* **25**, 801–817 (2015).
14. K. Chinthalapudi, V. Mandati, J. Zheng, A. J. Sharff, G. Bricogne, P. R. Griffin, J. Kissil, T. Izard, Lipid binding promotes the open conformation and tumor-suppressive activity of neurofibromin 2. *Nat. Commun.* **9**, 1338 (2018).
15. S. S. Scherer, D. H. Gutmann, Expression of the neurofibromatosis 2 tumor suppressor gene product, merlin, in Schwann cells. *J. Neurosci. Res.* **46**, 595–605 (1996).
16. N. Denisenko, C. Cifuentes-Diaz, T. Irinopoulou, M. Carnaud, E. Benoit, M. Niwa-Kawakita, F. Chareyre, M. Giovannini, J.-A. Girault, L. Goutebroze, Tumor suppressor schwannomin/merlin is critical for the organization of Schwann cell contacts in peripheral nerves. *J. Neurosci.* **28**, 10472–10481 (2008).
17. C. Gonzalez-Agosti, L. Xu, D. Pinney, R. Beauchamp, W. Hobbs, J. F. Gusella, V. R. Ramesh, The merlin tumor suppressor localizes preferentially in membrane ruffles. *Oncogene* **13**, 1239–1247 (1996).
18. J. T. Stickney, W. C. Bacon, M. Rojas, N. Ratner, W. Ip, Activation of the tumor suppressor merlin modulates its interaction with lipid rafts. *Cancer Res.* **64**, 2717–2724 (2004).
19. T. Mani, R. F. Hennigan, L. A. Foster, D. G. Conrady, A. B. Herr, W. Ip, FERM domain phosphoinositide binding targets merlin to the membrane and is essential for its growth-suppressive function. *Mol. Cell. Biol.* **31**, 1983–1996 (2011).
20. M. Curto, B. K. Cole, D. Lallemand, C.-H. Liu, A. I. McClatchey, Contact-dependent inhibition of EGFR signaling by Nf2/Merlin. *J. Cell Biol.* **177**, 893–903 (2007).
21. B. K. Cole, M. Curto, A. W. Chan, A. I. McClatchey, Localization to the cortical cytoskeleton is necessary for Nf2/merlin-dependent epidermal growth factor receptor silencing. *Mol. Cell. Biol.* **28**, 1274–1284 (2008).
22. D. Lallemand, J. Manent, A. Couvelard, A. Watilliaux, M. Siena, F. Chareyre, A. Lampin, M. Niwa-Kawakita, M. Kalamarides, M. Giovannini, Merlin regulates transmembrane receptor accumulation and signaling at the plasma membrane in primary mouse Schwann cells and in human schwannomas. *Oncogene* **28**, 854–865 (2009).
23. A. I. McClatchey, Merlin and ERM proteins: Unappreciated roles in cancer development? *Nat. Rev. Cancer* **3**, 877–883 (2003).
24. A. I. McClatchey, M. Giovannini, Membrane organization and tumorigenesis—The NF2 tumor suppressor, Merlin. *Genes Dev.* **19**, 2265–2277 (2005).
25. S. Maitra, R. M. Kulikauskas, H. Gavilan, R. G. Fehon, The tumor suppressors Merlin and Expanded function cooperatively to modulate receptor endocytosis and signaling. *Curr. Biol.* **16**, 702–709 (2006).
26. R. J. Shaw, J. G. Paez, M. Curto, A. Yaktine, W. M. Pruitt, I. Saotome, J. P. O'Bryan, V. Gupta, N. Ratner, C. J. Der, T. Jacks, A. I. McClatchey, The Nf2 tumor suppressor, merlin, functions in Rac-dependent signaling. *Dev. Cell* **1**, 63–72 (2001).
27. G.-H. Xiao, A. Beeser, J. Chernoff, J. R. Testa, p21-activated kinase links Rac/Cdc42 signaling to merlin. *J. Biol. Chem.* **277**, 883–886 (2002).
28. T. Okada, M. Lopez-Lago, F. G. Giancotti, Merlin/NF-2 mediates contact inhibition of growth by suppressing recruitment of Rac to the plasma membrane. *J. Cell Biol.* **171**, 361–371 (2005).
29. S. S. Houshmandi, R. J. Emnett, M. Giovannini, D. H. Gutmann, The neurofibromatosis 2 protein, merlin, regulates glial cell growth in an ErbB2- and Src-dependent manner. *Mol. Cell. Biol.* **29**, 1472–1486 (2009).
30. L. Zhou, E. Ercolano, S. Ammoun, M. C. Schmid, M. A. Barczyk, C. O. Hanemann, Merlin-deficient human tumors show loss of contact inhibition and activation of Wnt/β-catenin signaling linked to the PDGFR/Src and Rac/PAK pathways. *Neoplasia* **13**, 1101–1112 (2011).
31. H. Morrison, T. Sperka, J. Manent, M. Giovannini, H. Ponta, P. Herrlich, Merlin/neurofibromatosis type 2 suppresses growth by inhibiting the activation of Ras and Rac. *Cancer Res.* **67**, 520–527 (2007).
32. A. I. McClatchey, R. G. Fehon, Merlin and the ERM proteins--regulators of receptor distribution and signaling at the cell cortex. *Trends Cell Biol.* **19**, 198–206 (2009).
33. S. C. Hughes, R. G. Fehon, Phosphorylation and activity of the tumor suppressor Merlin and the ERM protein Moesin are coordinately regulated by the Slik kinase. *J. Cell Biol.* **175**, 305–313 (2006).
34. R. F. Hennigan, C. A. Moon, L. M. Parysek, K. R. Monk, G. Morfini, S. Berth, S. Brady, N. Ratner, The NF2 tumor suppressor regulates microtubule-based vesicle trafficking via a novel Rac, MLK and p38^{SAPK} pathway. *Oncogene* **32**, 1135–1143 (2013).
35. T. Muranen, M. Grönholm, A. Lampin, D. Lallemand, F. Zhao, M. Giovannini, O. Carpén, The tumor suppressor merlin interacts with microtubules and modulates Schwann cell microtubule cytoskeleton. *Hum. Mol. Genet.* **16**, 1742–1751 (2007).
36. L. B. Benseñor, K. Barlan, S. E. Rice, R. G. Fehon, V. I. Gelfand, Microtubule-mediated transport of the tumor-suppressor protein Merlin and its mutants. *Proc. Natl. Acad. Sci. U.S.A.* **107**, 7311–7316 (2010).
37. C. Yi, S. Troutman, D. Fera, A. Stemmer-Rachamimov, J. L. Avila, N. Christian, N. L. Persson, A. Shimono, D. W. Speicher, R. Marmorstein, L. Holmgren, J. L. Kissil, A tight junction-associated Merlin-angiomotin complex mediates Merlin's regulation of mitogenic signaling and tumor suppressive functions. *Cancer Cell* **19**, 527–540 (2011).
38. M. Kressel, B. Schmucker, Nucleocytoplasmic transfer of the NF2 tumor suppressor protein merlin is regulated by exon 2 and a CRM1-dependent nuclear export signal in exon 15. *Hum. Mol. Genet.* **11**, 2269–2278 (2002).
39. T. Muranen, M. Grönholm, G. H. Renkema, O. Carpén, Cell cycle-dependent nucleocytoplasmic shuttling of the neurofibromatosis 2 tumour suppressor merlin. *Oncogene* **24**, 1150–1158 (2005).
40. W. Li, L. You, J. Cooper, G. Schiavon, A. Pepe-Caprio, L. Zhou, R. Ishii, M. Giovannini, C. O. Hanemann, S. B. Long, H. Erdjument-Bromage, P. Zhou, P. Tempst, F. G. Giancotti, Merlin/NF2 suppresses tumorigenesis by inhibiting the E3 ubiquitin ligase CRL4^{DCAF1} in the nucleus. *Cell* **140**, 477–490 (2010).
41. J. Cooper, W. Li, L. You, G. Schiavon, A. Pepe-Caprio, L. Zhou, R. Ishii, M. Giovannini, C. O. Hanemann, S. B. Long, H. Erdjument-Bromage, P. Zhou, P. Tempst, F. G. Giancotti,

Merlin/NF2 functions upstream of the nuclear E3 ubiquitin ligase $CRL4^{DCAF1}$ to suppress oncogenic gene expression. *Sci. Signal.* **4**, pt6 (2011).
42. F. Hamaratoglu, M. Willecke, M. Kango-Singh, R. Nolo, E. Hyun, C. Tao, H. Jafar-Nejad, G. Halder, The tumour-suppressor genes NF2/Merlin and Expanded act through Hippo signalling to regulate cell proliferation and apoptosis. *Nat. Cell Biol.* **8**, 27–36 (2006).
43. F. Yin, J. Yu, Y. Zheng, Q. Chen, N. Zhang, D. Pan, Spatial organization of Hippo signaling at the plasma membrane mediated by the tumor suppressor Merlin/NF2. *Cell* **154**, 1342–1355 (2013).
44. I. M. Moya, G. Halder, Discovering the Hippo pathway protein-protein interactome. *Cell Res.* **24**, 137–138 (2014).
45. Y. Kwon, A. Vinayagam, X. Sun, N. Dephoure, S. P. Gygi, P. Hong, N. Perrimon, The Hippo signaling pathway interactome. *Science* **342**, 737–740 (2013).
46. A. L. Couzens, J. D. R. Knight, M. J. Kean, G. Teo, A. Weiss, W. H. Dunham, Z.-Y. Lin, R. D. Bagshaw, F. Sicheri, T. Pawson, J. L. Wrana, H. Choi, A.-C. Gingras, Protein interaction network of the mammalian Hippo pathway reveals mechanisms of kinase-phosphatase interactions. *Sci. Signal.* **6**, rs15 (2013).
47. D. R. Scoles, The merlin interacting proteins reveal multiple targets for NF2 therapy. *Biochim. Biophys. Acta* **1785**, 32–54 (2008).
48. D. Lallemand, M. Curto, I. Saotome, M. Giovannini, A. I. McClatchey, NF2 deficiency promotes tumorigenesis and metastasis by destabilizing adherens junctions. *Genes Dev.* **17**, 1090–1100 (2003).
49. V. J. Obremski, A. M. Hall, C. Fernández-Valle, Merlin, the neurofibromatosis type 2 gene product, and beta1 integrin associate in isolated and differentiating Schwann cells. *J. Neurobiol.* **37**, 487–501 (1998).
50. C. Flaiz, T. Utermark, D. B. Parkinson, A. Poetsch, C. O. Hanemann, Impaired intercellular adhesion and immature adherens junctions in merlin-deficient human primary schwannoma cells. *Glia* **56**, 506–515 (2008).
51. E. de Boer, P. Rodriguez, E. Bonte, J. Krijgsveld, E. Katsantoni, A. Heck, F. Grosveld, J. Strouboulis, Efficient biotinylation and single-step purification of tagged transcription factors in mammalian cells and transgenic mice. *Proc. Natl. Acad. Sci. U.S.A.* **100**, 7480–7485 (2003).
52. I. Sher, C. O. Hanemann, P. A. Karplus, A. Bretscher, The tumor suppressor merlin controls growth in its open state, and phosphorylation converts it to a less-active more-closed state. *Dev. Cell* **22**, 703–705 (2012).
53. M. C. Wilkes, C. E. Repellin, M. Hong, M. Bracamonte, S. G. Penheiter, J.-P. Borg, E. B. Leof, Erbin and the NF2 tumor suppressor Merlin cooperatively regulate cell-type-specific activation of PAK2 by TGF-β. *Dev. Cell* **16**, 433–444 (2009).
54. R. Rangwala, F. Banine, J.-P. Borg, L. S. Sherman, Erbin regulates mitogen-activated protein (MAP) kinase activation and MAP kinase-dependent interactions between Merlin and adherens junction protein complexes in Schwann cells. *J. Biol. Chem.* **280**, 11790–11797 (2005).
55. J.-M. Dong, F. P.-L. Tay, H. L.-F. Swa, J. Gunaratne, T. Leung, B. Burke, E. Manser, Proximity biotinylation provides insight into the molecular composition of focal adhesions at the nanometer scale. *Sci. Signal.* **9**, rs4 (2016).
56. C. M. Van Itallie, A. J. Tietgens, A. Aponte, K. Fredriksson, A. S. Fanning, M. Gucek, J. M. Anderson, Biotin ligase tagging identifies proteins proximal to E-cadherin, including lipoma preferred partner, a regulator of epithelial cell-cell and cell-substrate adhesion. *J. Cell Sci.* **127**, 885–895 (2014).
57. C. M. Van Itallie, A. Aponte, A. J. Tietgens, M. Gucek, K. Fredriksson, J. M. Anderson, The N and C termini of ZO-1 are surrounded by distinct proteins and functional protein networks. *J. Biol. Chem.* **288**, 13775–13788 (2013).
58. M. P. Hall, J. Unch, B. F. Binkowski, M. P. Valley, B. L. Butler, M. G. Wood, P. Otto, K. Zimmerman, G. Vidugiris, T. Machleidt, M. B. Robers, H. A. Benink, C. T. Eggers, M. R. Slater, P. L. Meisenheimer, D. H. Klaubert, F. Fan, L. P. Encell, K. V. Wood, Engineered luciferase reporter from a deep sea shrimp utilizing a novel imidazopyrazinone substrate. *ACS Chem. Biol.* **7**, 1848–1857 (2012).
59. C. Royer, S. Koch, X. Qin, J. Zak, L. Buti, E. Dudziec, S. Zhong, I. Ratnayaka, S. Srinivas, X. Lu, ASPP2 links the apical lateral polarity complex to the regulation of YAP activity in epithelial cells. *PLOS ONE* **9**, e111384 (2014).
60. B. Deguen, P. Mérel, L. Goutebroze, M. Giovannini, H. Reggio, M. Arpin, G. K. Thomas, Impaired interaction of naturally occurring mutant NF2 protein with actin-based cytoskeleton and membrane. *Hum. Mol. Genet.* **7**, 217–226 (1998).
61. J. Yu, Y. Zheng, J. Dong, S. Klusza, W.-M. Deng, D. Pan, Kibra functions as a tumor suppressor protein that regulates Hippo signaling in conjunction with Merlin and Expanded. *Dev. Cell* **18**, 288–299 (2010).
62. D. Jukam, C. Desplan, Binary regulation of Hippo pathway by Merlin/NF2, Kibra, Lgl, and Melted specifies and maintains postmitotic neuronal fate. *Dev. Cell* **21**, 874–887 (2011).
63. B. V. V. G. Reddy, K. D. Irvine, Regulation of *Drosophila* glial cell proliferation by Merlin-Hippo signaling. *Development* **138**, 5201–5212 (2011).
64. B. Zhao, L. Li, Q. Lu, L. H. Wang, C.-Y. Liu, Q. Lei, K.-L. Guan, Angiomotin is a novel Hippo pathway component that inhibits YAP oncoprotein. *Genes Dev.* **25**, 51–63 (2011).
65. J.-P. Lambert, M. Tucholska, C. Go, J. D. R. Knight, A.-C. Gingras, Proximity biotinylation and affinity purification are complementary approaches for the interactome mapping of chromatin-associated protein complexes. *J. Proteomics* **118**, 81–94 (2015).
66. P. Lönn, U. Landegren, Close encounters—Probing proximal proteins in live or fixed cells. *Trends Biochem. Sci.* **42**, 504–515 (2017).
67. F. A. Court, J. E. Hewitt, K. Davies, B. L. Patton, A. Uncini, L. Wrabetz, M. L. Feltri, A laminin-2, dystroglycan, utrophin axis is required for compartmentalization and elongation of myelin segments. *J. Neurosci.* **29**, 3908–3919 (2009).
68. R. J. Shaw, A. I. McClatchey, T. Jacks, Localization and functional domains of the neurofibromatosis type II tumor suppressor, merlin. *Cell Growth Differ.* **9**, 287–296 (1998).
69. B. Schmucker, W. G. Ballhausen, M. Kressel, Subcellular localization and expression pattern of the neurofibromatosis type 2 protein merlin/schwannomin. *Eur. J. Cell Biol.* **72**, 46–53 (1997).
70. T. Y. El Sayegh, P. D. Arora, K. Ling, C. Laschinger, P. A. Janmey, R. A. Anderson, C. A. McCulloch, Phosphatidylinositol-4,5 bisphosphate produced by PIP5KIγ regulates gelsolin, actin assembly, and adhesion strength of N-cadherin junctions. *Mol. Biol. Cell* **18**, 3026–3038 (2007).
71. H. Qu, Y. Tu, X. Shi, H. Larjava, M. A. Saleem, S. J. Shattil, K. Fukuda, J. Qin, M. Kretzler, C. Wu, Kindlin-2 regulates podocyte adhesion and fibronectin matrix deposition through interactions with phosphoinositides and integrins. *J. Cell Sci.* **124**, 879–891 (2011).
72. G. M. Goñi, C. Epifano, J. Boskovic, M. Camacho-Artacho, J. Zhou, A. Bronowska, M. T. Martin, M. J. Eck, L. Kremer, F. Grater, F. L. Gervasio, M. Perez-Moreno, D. Lietha, Phosphatidylinositol 4,5-bisphosphate triggers activation of focal adhesion kinase by inducing clustering and conformational changes. *Proc. Natl. Acad. Sci. U.S.A.* **111**, E3177–E3186 (2014).
73. M. Fukumoto, T. Ijuin, T. Takenawa, $PI(3,4)P_2$ plays critical roles in the regulation of focal adhesion dynamics of MDA-MB-231 breast cancer cells. *Cancer Sci.* **108**, 941–951 (2017).
74. S. Ghosh, C. Huber, Q. Siour, S. B. Sousa, M. Wright, V. Cormier-Daire, C. Erneux, Fibroblasts derived from patients with opsismodysplasia display SHIP2-specific cell migration and adhesion defects. *Hum. Mutat.* **38**, 1731–1739 (2017).
75. S. K. Thukral, G. C. Blain, K. K. Chang, S. Fields, Distinct residues of human p53 implicated in binding to DNA, simian virus 40 large T antigen, 53BP1, and 53BP2. *Mol. Cell. Biol.* **14**, 8315–8321 (1994).
76. K. Iwabuchi, B. Li, H. F. Massa, B. J. Trask, T. Date, S. Fields, Stimulation of p53-mediated transcriptional activation by the p53-binding proteins, 53BP1 and 53BP2. *J. Biol. Chem.* **273**, 26061–26068 (1998).
77. V. Vives, J. Su, S. Zhong, I. Ratnayaka, E. Slee, R. Goldin, X. Lu, ASPP2 is a haploinsufficient tumor suppressor that cooperates with p53 to suppress tumor growth. *Genes Dev.* **20**, 1262–1267 (2006).
78. Y. Wang, N. Godin-Heymann, X. Dan Wang, D. Bergamaschi, S. Llanos, X. Lu, ASPP1 and ASPP2 bind active RAS, potentiate RAS signalling and enhance p53 activity in cancer cells. *Cell Death Differ.* **20**, 525–534 (2013).
79. H. Benyamini, H. Leonov, S. Rotem, C. Katz, I. T. Arkin, A. Friedler, A model for the interaction between NF-kappa-B and ASPP2 suggests an I-kappa-B-like binding mechanism. *Proteins* **77**, 602–611 (2009).
80. L. Naumovski, M. L. Cleary, The p53-binding protein 53BP2 also interacts with Bc12 and impedes cell cycle progression at G2/M. *Mol. Cell. Biol.* **16**, 3884–3892 (1996).
81. R. Gemayel, S. Chavali, K. Pougach, M. Legendre, B. Zhu, S. Boeynaems, E. van der Zande, K. Gevaert, F. Rousseau, J. Schymkowitz, M. M. Babu, K. J. Verstrepen, Variable glutamine-rich repeats modulate transcription factor activity. *Mol. Cell* **59**, 615–627 (2015).
82. J. L. Kissil, K. C. Johnson, M. S. Eckman, T. Jacks, Merlin phosphorylation by p21-activated kinase 2 and effects of phosphorylation on merlin localization. *J. Biol. Chem.* **277**, 10394–10399 (2002).
83. V. Vasioukhin, Adherens junctions and cancer. *Subcell. Biochem.* **60**, 379–414 (2012).
84. T. A. Martin, The role of tight junctions in cancer metastasis. *Semin. Cell Dev. Biol.* **36**, 224–231 (2014).
85. Y. Wallez, P. Huber, Endothelial adherens and tight junctions in vascular homeostasis, inflammation and angiogenesis. *Biochim. Biophys. Acta* **1778**, 794–809 (2008).
86. B. Boggetti, C. M. Niessen, Adherens junctions in mammalian development, homeostasis and disease: Lessons from mice. *Subcell. Biochem.* **60**, 321–355 (2012).
87. M. A. Schwartz, D. W. Simone, Cell adhesion receptors in mechanotransduction. *Curr. Opin. Cell Biol.* **20**, 551–556 (2008).
88. C. Chiasson-MacKenzie, Z. S. Morris, Q. Baca, B. Morris, J. K. Coker, R. Mirchev, A. E. Jensen, T. Carey, S. L. Stott, D. E. Golan, A. I. McClatchey, NF2/Merlin mediates contact-dependent inhibition of EGFR mobility and internalization via cortical actomyosin. *J. Cell Biol.* **211**, 391–405 (2015).
89. T. Das, K. Safferling, S. Rausch, N. Grabe, H. Boehm, J. P. Spatz, A molecular mechanotransduction pathway regulates collective migration of epithelial cells. *Nat. Cell Biol.* **17**, 276–287 (2015).
90. M. K. Han, J. de Rooij, Converging and unique mechanisms of mechanotransduction at adhesion sites. *Trends Cell Biol.* **26**, 612–623 (2016).

91. B. Zhao, X. Wei, W. Li, R. S. Udan, Q. Yang, J. Kim, J. Xie, T. Ikenoue, J. Yu, L. Li, P. Zheng, K. Ye, A. Chinnaiyan, G. Halder, Z.-C. Lai, K.-L. Guan, Inactivation of YAP oncoprotein by the Hippo pathway is involved in cell contact inhibition and tissue growth control. *Genes Dev.* **21**, 2747–2761 (2007).
92. A. Bratt, O. Birot, I. Sinha, N. Veitonmäki, K. Aase, M. Ernkvist, L. Holmgren, Angiomotin regulates endothelial cell-cell junctions and cell motility. *J. Biol. Chem.* **280**, 34859–34869 (2005).
93. H. Sabra, M. Brunner, V. Mandati, B. Wehrle-Haller, D. Lallemand, A.-S. Ribba, G. Chevalier, P. Guardiola, M. R. Block, D. Bouvard, β1 integrin-dependent Rac/group I PAK signaling mediates YAP activation of Yes-associated protein 1 (YAP1) via NF2/merlin. *J. Biol. Chem.* **292**, 19179–19197 (2017).
94. K. T. Furukawa, K. Yamashita, N. Sakurai, S. Ohno, The epithelial circumferential actin belt regulates YAP/TAZ through nucleocytoplasmic shuttling of merlin. *Cell Rep.* **20**, 1435–1447 (2017).
95. M. Buchert, C. Poon, J. A. J. King, T. Baechi, G. D'Abaco, F. Hollande, C. M. Hovens, AF6/s-afadin is a dual residency protein and localizes to a novel subnuclear compartment. *J. Cell. Physiol.* **210**, 212–223 (2007).
96. M. Polette, M. Mestdagt, S. Bindels, B. Nawrocki-Raby, W. Hunziker, J. M. Foidart, P. Birembaut, C. Gilles, Beta-catenin and ZO-1: Shuttle molecules involved in tumor invasion-associated epithelial-mesenchymal transition processes. *Cells Tissues Organs* **185**, 61–65 (2007).
97. R. K. Kutty, S. Chen, W. Samuel, C. Vijayasarathy, T. Duncan, J.-Y. Tsai, R. N. Fariss, D. Carper, C. Jaworski, B. Wiggert, Cell density-dependent nuclear/cytoplasmic localization of NORPEG (RAI14) protein. *Biochem. Biophys. Res. Commun.* **345**, 1333–1341 (2006).
98. H. Uhlmann-Schiffler, S. Kiermayer, H. Stahl, The DEAD box protein Ddx42p modulates the function of ASPP2, a stimulator of apoptosis. *Oncogene* **28**, 2065–2073 (2009).
99. P. I. Poulikakos, G.-H. Xiao, R. Gallagher, S. Jablonski, S. C. Jhanwar, J. R. Testa, Re-expression of the tumor suppressor NF2/merlin inhibits invasiveness in mesothelioma cells and negatively regulates FAK. *Oncogene* **25**, 5960–5968 (2006).
100. J. Zhou, C. Aponte-Santamaria, S. Sturm, J. T. Bullerjahn, A. Bronowska, F. Grater, Mechanism of focal adhesion kinase mechanosensing. *PLOS Comput. Biol.* **11**, e1004593 (2015).
101. D. E. Dostal, H. Feng, D. Nizamutdinov, H. B. Golden, S. H. Afroze, J. D. Dostal, J. C. Jacob, D. M. Foster, C. Tong, S. Glaser, F. N. U. Gerilechaogetu, Mechanosensing and regulation of cardiac function. *J. Clin. Exp. Cardiolog.* **5**, 314 (2014).
102. M. Gregor, S. Osmanagic-Myers, G. Burgstaller, M. Wolfram, I. Fischer, G. Walko, G. P. Resch, A. Jörgl, H. Herrmann, G. Wiche, Mechanosensing through focal adhesion-anchored intermediate filaments. *FASEB J.* **28**, 715–729 (2014).
103. W. C. Wei, H. H. Lin, M. R. Shen, M. J. Tang, Mechanosensing machinery for cells under low substratum rigidity. *Am. J. Physiol. Cell Physiol.* **295**, C1579–C1589 (2008).
104. H.-B. Wang, M. Dembo, S. K. Hanks, Y.-l. Wang, Focal adhesion kinase is involved in mechanosensing during fibroblast migration. *Proc. Natl. Acad. Sci. U.S.A.* **98**, 11295–11300 (2001).
105. N. R. Shah, I. Tancioni, K. K. Ward, C. Lawson, X. L. Chen, C. Jean, F. J. Sulzmaier, S. Uryu, N. L. G. Miller, D. C. Connolly, D. D. Schlaepfer, Analyses of merlin/NF2 connection to FAK inhibitor responsiveness in serous ovarian cancer. *Gynecol. Oncol.* **134**, 104–111 (2014).
106. I. M. Shapiro, V. N. Kolev, C. M. Vidal, Y. Kadariya, J. E. Ring, Q. Wright, D. T. Weaver, C. Menges, M. Padval, A. I. McClatchey, Q. Xu, J. R. Testa, J. A. Pachter, Merlin deficiency predicts FAK inhibitor sensitivity: A synthetic lethal relationship. *Sci. Transl. Med.* **6**, 237ra68 (2014).
107. S. Nakata, N. Fujita, Y. Kitagawa, R. Okamoto, H. Ogita, Y. Takai, Regulation of platelet-derived growth factor receptor activation by afadin through SHP-2: Implications for cellular morphology. *J. Biol. Chem.* **282**, 37815–37825 (2007).
108. Z. Wang, Y. Liu, M. Takahashi, K. Van Hook, K. M. Kampa-Schittenhelm, B. C. Sheppard, R. C. Sears, P. J. S. Stork, C. D. Lopez, N terminus of ASPP2 binds to Ras and enhances Ras/Raf/MEK/ERK activation to promote oncogene-induced senescence. *Proc. Natl. Acad. Sci. U.S.A.* **110**, 312–317 (2013).
109. K. J. Roux, D. I. Kim, M. Raida, B. Burke, A promiscuous biotin ligase fusion protein identifies proximal and interacting proteins in mammalian cells. *J. Cell Biol.* **196**, 801–810 (2012).
110. J. Reimand, M. Kull, H. Peterson, J. Hansen, J. Vilo, g:Profiler—A web-based toolset for functional profiling of gene lists from large-scale experiments. *Nucleic Acids Res.* **35**, W193–W200 (2007).
111. T. Hulsen, J. de Vlieg, W. Alkema, BioVenn—A web application for the comparison and visualization of biological lists using area-proportional Venn diagrams. *BMC Genomics* **9**, 488 (2008).
112. M. Kutmon, M. P. van Iersel, A. Bohler, T. Kelder, N. Nunes, A. R. Pico, C. T. Evelo, PathVisio 3: An extendable pathway analysis toolbox. *PLOS Comput. Biol.* **11**, e1004085 (2015).
113. E. W. Deutsch, A. Csordas, Z. Sun, A. Jarnuczak, Y. Perez-Riverol, T. Ternent, D. S. Campbell, M. Bernal-Llinares, S. Okuda, S. Kawano, R. L. Moritz, J. J. Carver, M. Wang, Y. Ishihama, N. Bandeira, H. Hermjakob, J. A. Vizcaíno, The ProteomeXchange consortium in 2017: Supporting the cultural change in proteomics public data deposition. *Nucleic Acids Res.* **45**, D1100–D1106 (2017).

Acknowledgments: We thank M. Bogart, M. Carroll, and N. Olsen for expert technical assistance and R. Coover (Cincinnati Children's Hospital), B. Ozanne, and S.C.M. Tedesco for critical reading of the manuscript. **Funding:** This work was supported by the Department of Defense, Congressionally Directed Medical Research Program Awards NF120118 and NF160078 (to R.F.H.) and a National Institutes of Health Jacob Javits Merit Award NINDS (R37 NS083580) (to N.R.). **Author contributions:** R.F.H. designed and conducted most experiments. J.S.F. assisted in data analysis. S.G. performed microscopy. N.R. contributed to experimental design, data analysis, and manuscript preparation. **Competing interests:** The authors declare that they have no competing interests. **Data and materials availability:** The MS proteomics data have been deposited to the ProteomeXchange Consortium via the PRIDE (*113*) partner repository with the dataset identifier PXD012017. All data associated with this study are present in the paper are present in the paper or the Supplementary Materials.

Submitted 23 July 2018
Accepted 28 March 2019
Published 23 April 2019
10.1126/scisignal.aau8749

Citation: R. F. Hennigan, J. S. Fletcher, S. Guard, N. Ratner, Proximity biotinylation identifies a set of conformation-specific interactions between Merlin and cell junction proteins. *Sci. Signal.* **12**, eaau8749 (2019).

Science Signaling

Proximity biotinylation identifies a set of conformation-specific interactions between Merlin and cell junction proteins

Robert F. Hennigan, Jonathan S. Fletcher, Steven Guard and Nancy Ratner

Sci. Signal. **12** (578), eaau8749.
DOI: 10.1126/scisignal.aau8749

The Merlin interactome identifies cell junction proteins

Merlin (also called NF2) is a tumor suppressor that associates with lipid rafts and cell junctions. To identify potential Merlin binding partners, Hennigan *et al.* performed proximity biotinylation assays in murine Schwann cells with wild-type and various mutant forms of Merlin that could not associate with the plasma membrane or were locked in different conformations. Fewer proteins interacted with the form of Merlin that could not associate with the plasma membrane, and some proteins interacted specifically with the closed conformation. Most of the Merlin-proximal proteins were components of or associated with cell junctions and focal adhesions. Among the previously unidentified Merlin-interacting proteins was the tumor suppressor ASPP2 (also called Tp53bp2), which bound directly to the closed conformation. This dataset confirms cell junctions as important sites for Merlin activity and reveals additional binding partners.

Science Signaling (ISSN 1937-9145) is published by the American Association for the Advancement of Science, 1200 New York Avenue NW, Washington, DC 20005. The title *Science Signaling* is a registered trademark of AAAS.